Journal of Green Energy Research and Innovation

Applying Sliding Mode Control Along with Particle Swarm Algorithm in Order to Optimally Control the System Wind Turbines with Variable Speed

Sasan Pirouzi, Ali Naderi

Highlights

- MPP tracking while observing the allowed range of duty cycle
- Preserving the permissible range of ripples of various parameters
- Extending the operating range of the variable-resistance method
- Adopting the proposed method for PV energy management

Graphical Abstract

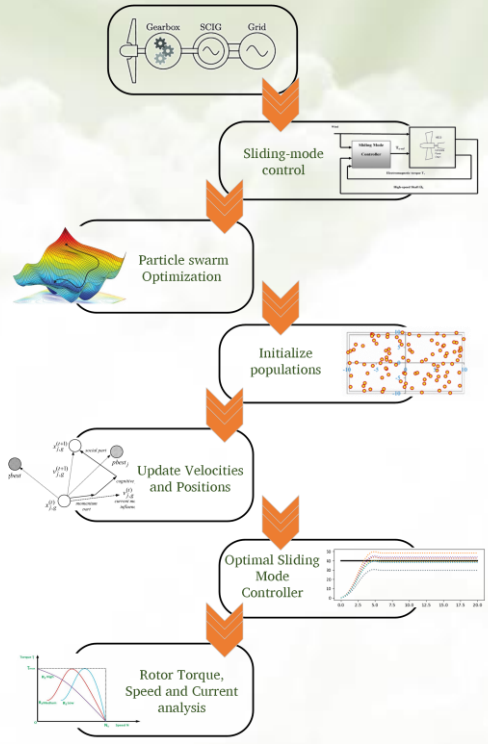

Use your device to scan and read the article online

Citation

S. Pirouzi, and A. Naderi, "Applying Sliding Mode Control Along with Particle Swarm Algorithm in Order to Optimally Control the System Wind Turbines with Variable Speed," *Journal of Green Energy Research and Innovation*, vol. 1, no. 2, pp. 64-80, 2024.

https://doi.org/10.61186/jgeri.1.2.64

JGERI Journal of Green Energy Research and Innovation

Online ISSN: 3041-9018

Journal of Green Energy Research and Innovation

Journal Homepage: www.jgeri.araku.ac.ir

Applying Sliding Mode Control Along with Particle Swarm Algorithm in Order to Optimally Control the System Wind Turbines with Variable Speed

Sasan Pirouzi [1]*, Ali Naderi [2]

[1] *Islamic Azad University of Semmirom Branch, Semmirom, Iran.*
[2] *Department of Engineering, Yazd University, Yazd, Iran.*

* ***Corresponding Author:*** *s.pirouzi@sutech.ac.ir*

ARTICLE INFO

Keywords:
Wind turbine,
Sliding mode control,
Particle swarm algorithm.

Article history:
Received: 04 February 2024;
Revised: 01 March 2024;
Accepted: 06 March 2024;

Article type:
Research Article

ABSTRACT

The utilization of renewables is developing rapidly due to environmental issues and a lack of fuel fossils. In this regard, wind turbines, as a type of renewable energy source, have been widely adopted in the power system thanks to their higher power generation capacity. Numerous methods have been introduced so far to control wind turbines, which are essential in generating wind energy. The sliding mode control, because of its unique features like being resistant to external disturbances, dynamics unmodeled and uncertainty, the relative simplicity of the control law, a relatively small amount of calculations, and straightforward implementation, is amongst the most preferred control designs in this realm. In this study, the control strategy is based on a combination of sliding mode and particle swarm optimization and is applied to a wind turbine with a grid-connected squirrel cage induction generator. The proposed method maximizes the power output of the wind turbine by limiting small changes in the electromagnetic torque. The main goal of the suggested design is to reduce the squared error of the electromagnetic torque, rotor speed, and stator current. The sliding mode control for the wind turbine helps obtain optimal values for the parameters of the design.

1. Introduction

1.1. Modified quadratic power curve

The use of renewable energy sources is expanding rapidly due to environmental concerns and the depletion of fossil fuels [1-3]. Among these sources, wind turbines have attracted considerable attention over other renewable technologies because of their significant power generation potential [4-5]. Wind turbines can be categorized based on their operational speed into two types: fixed and variable speed [6-7]. Variable-speed wind turbines offer numerous advantages over their fixed-speed counterparts, including the ability to align the generator shaft speed with varying wind speeds. Several control methods have been proposed by researchers to optimize turbine performance. For instance, some have developed a feedback controller for the system using linear control methods. These approaches rely on linearizing the wind turbine model, simplifying the

turbine equations, and designing the controller, which can simplify the analytical solution. However, linear controllers are limited by the wind turbine's nonlinear characteristics and cannot achieve the desired optimal performance due to these limitations and nonlinear behaviors. Sliding mode control, known for its robustness to external disturbances, unmodeled dynamics, and uncertainties, along with the simplicity of its control law and minimal computational requirements, emerges as an ideal solution for controlling nonlinear, multivariable systems like wind turbines. Thus, sliding mode control is considered by many researchers as the preferred method for achieving optimal turbine control.

1.2. Research background

Ref. [8] discusses the high-order sliding mode control method due to features such as reducing external mechanical stress, limited arrival time, and resistance to external and dynamic disturbances, including unmodeled ones. This article utilizes a 2nd order vector slip surface to generate control signals. It employs rotor current and electric torque to maximize output power without damaging the system. Article [9] explores control of production power in turbines, acknowledging that wind speeds vary. It introduces a system with two working areas dependent on peak speed, utilizing a high-degree sliding mode control method to ensure system stability in both areas and to apply ideal feedback control. Despite model uncertainties, this control method demonstrates resistance to system parameter uncertainties. It calculates the speed of the rotor and its torque via a sliding mode observer, and the difference from the optimal torque is used as the control error. A sliding mode modulator is employed to control the output power. Another approach for controlling the generator [10], is the adaptive fuzzy integral variable structure controller, aimed at maximizing wind power by adjusting turbine speed based on wind speed. This surpasses traditional control methods reliant on mathematical models. It introduces an adaptive fuzzy integral variable structure for control. The combination of a robust nonlinear controller with quadratic sliding mode control [11] represents another strategy for turbine control. This method integrates a robust nonlinear controller with a quadratic sliding mode method, known as the strong convolution algorithm, to manage the wind turbine system. The goal is to maximize wind energy captured by the turbine and maintain the stator power factor of a wire rotor induction generator at a desired level. Ref. [12] proposes a method to control generator speed, presenting a variable-speed wind turbine power control method connected to the grid. Another study combines integral variable structure control and directional field vector to manage rotor voltage, subsequently controlling rotor current and stator voltage [13]. To address the buzzing phenomenon, a saturation function replaces the sign function. Additionally, to minimize steady-state error, an integral sliding surface is employed, which overall achieves our objectives for the smoothness and safety of the generator in controlling no-load disconnection.

In another approach, sliding mode control is utilized for bending angle control due to its fast response, minimal lift, and resistance to disturbances. However, the sliding mode method often encounters the issue of creating a buzzing phenomenon. This article

mitigates the problem through the use of a pseudo-sliding mode generator, showcasing that the control agent employed offers higher efficiency compared to traditional integral controllers [14]. Ref. [15] discusses a control strategy employing a nonlinear flow on the turbine for variable-speed wind turbines with dual induction generators. Ref. [16] presents an enhanced direct power control method for grid-connected wind turbines, especially when facing unbalanced grid voltages. Furthermore, Ref. [17] explores the application of second-order sliding mode control for synchronous power control in networking.

1.3. Research gaps and contributions

Control of wind turbines using sliding mode control is sparsely covered in existing research. This method, notable for its distinct capabilities, is the focus of this paper. Sliding mode control is characterized by its variable structure, rapidly switching between multiple control strategies. The initial design step involves selecting a suitable sliding surface, crucial for modeling the system's optimal closed-loop performance in the variable state space. Subsequent steps include determining the paths for system control to ensure it remains within the desired trajectory [18]. The design of a sliding mode controller for wind turbines, especially variable speed ones, prioritizes ensuring effective performance and control stability. As demonstrated in Figure 1, this paper utilizes a smart particle swarm algorithm to optimize the parameters of the sliding surface function for sliding mode control. It's worth mentioning that the approach outlined in this paper potentially maximizes the power harvested from the wind turbine by minimizing fluctuations in electromagnetic torque. Essentially, this paper proposes a control strategy that merges sliding mode control with an optimal algorithm, specifically particle swarm optimization, applied to a grid-connected wind turbine with a squirrel cage induction generator. This strategy aims to achieve two objectives. The primary goal is to maximize the wind power captured by the turbine, while the secondary goal, pursued concurrently, is to minimize changes in electromagnetic torque. The innovation and features of this approach are highlighted as follows:

- Using the sliding mode control for the wind turbine to obtain the maximum power from the wind system.
- Determining the optimal values of the parameters of the sliding surface function of the sliding mode control for the optimal performance of the wind turbine.

Next, the proposed design model for the wind turbine is detailed in the second part. Following that, the third part provides numerical results to assess the effectiveness of the proposed design. Finally, the fourth part discusses the overall implications of the results.

2. Wind turbine model

Figures 1 and 2 present the comprehensive block diagram of the system under study, which is a variable speed squirrel cage induction generator (SCIG) controlled via sliding mode. Additionally, the parameters of the sliding mode controller are optimized using the Particle Swarm Optimization (PSO) algorithm, thereby assessing its optimal

configuration. Consequently, the model of the wind power plant, the sliding mode controller, and the PSO algorithm are detailed in the subsequent sections.

2.1. Wind energy conversion system model

Based on Figure 2, the important components of a variable-speed wind turbine are:

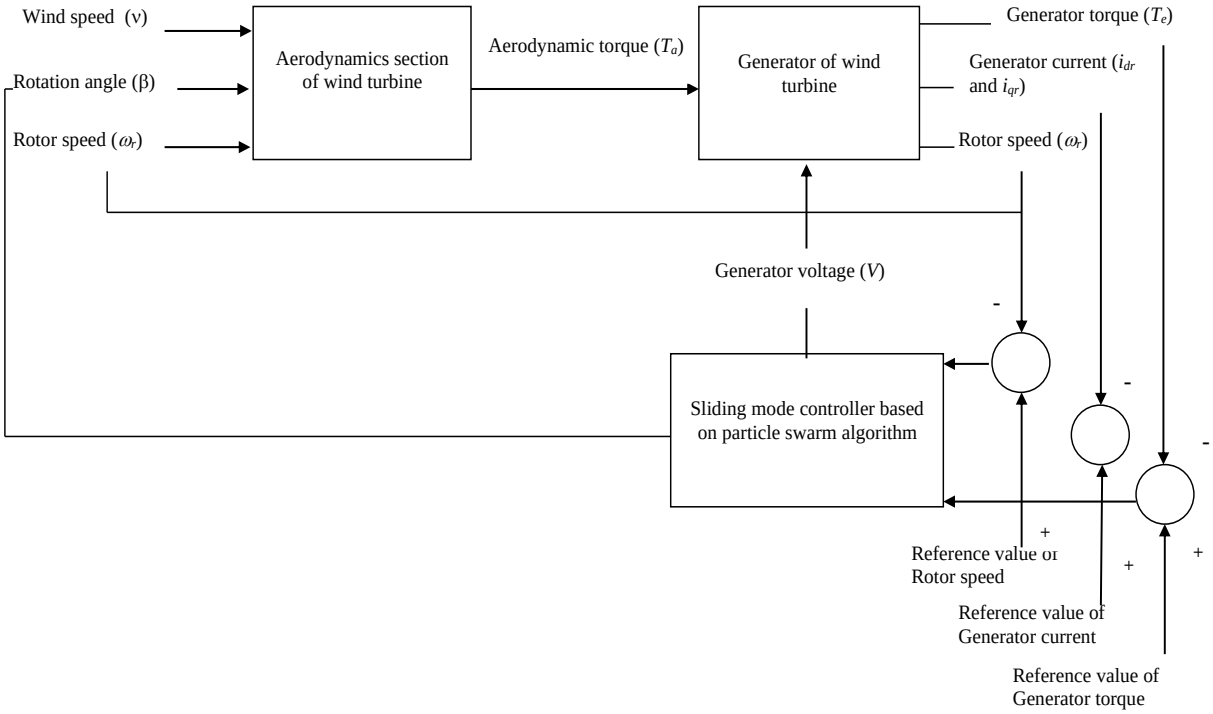

Figure 1. General of the proposed plan.

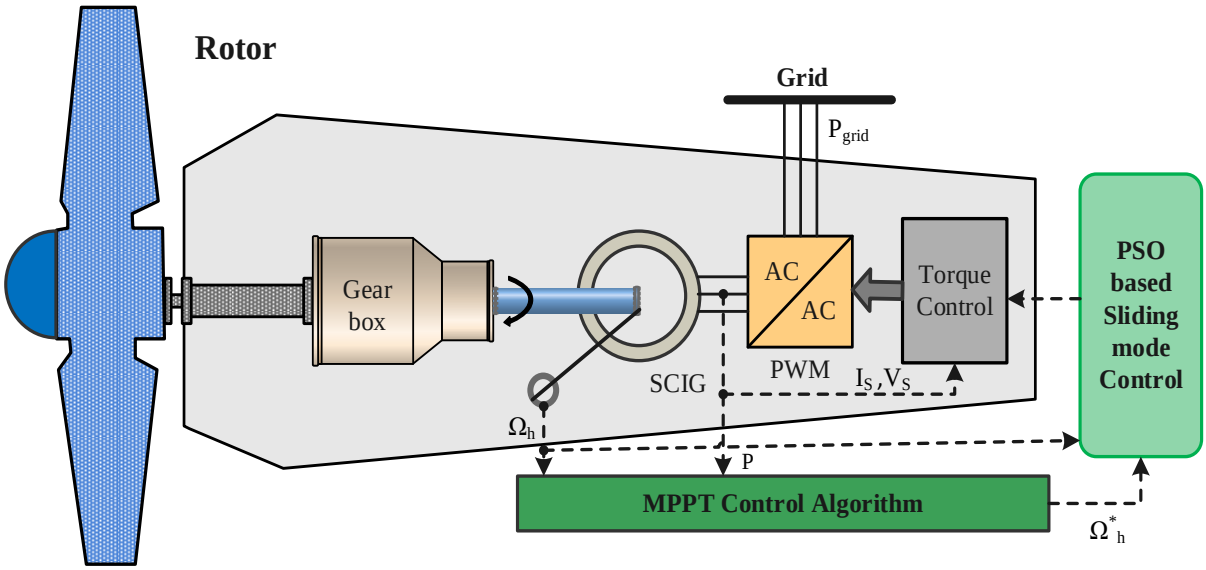

Figure 2. Wind energy conversion system based on SCIG.

1- Turbine
2- gearbox
3- Squirrel rack induction generator (SCIG) connected to the grid

Therefore, in the following, the mathematical model of these components will be presented in order, which expresses their behavior in the studied system.

A) wind turbine model (aerodynamic section) Wind turbine *generally* converts the kinetic energy of the wind into mechanical energy slowly and also the total energy available from the wind turbine can be calculated from Equation (1):

$$E_k = \frac{1}{2}mv^2 \tag{1}$$

where (m) represents the mass of air passing through a square disk of one square meter, and (v) denotes the wind speed, expressed in meters per second. It should be noted that the air mass can also be calculated from Equation (2):

$$m = \rho Ad \tag{2}$$

In Equation (2), (ρ) represents the air density, (A) denotes the area swept by the turbine blades, and (d) is the distance from the wind source. According to Betz's theory, the mechanical power extractable from the wind turbine (P_a) can be calculated using the form of Equation (3):

$$P_a = \frac{1}{2}\rho\pi R^2 v^3 C_p(\lambda,\beta) \tag{3}$$

where (R) is the radius of the wind turbine blade, (λ) represents the tip speed ratio, and (β) denotes the pitch angle, referring to the angle between the chord of the blade and the plane of rotation. Finally, (C_p) is the power coefficient of the wind turbine. It is noteworthy that the tip speed ratio is given by Equation (4):

$$\lambda = \frac{\omega_r R}{v} \tag{4}$$

(ω_r) is the rotational speed of the wind turbine rotor. It should be noted that Ref. [19] has derived a mathematical relationship for (C_p), which is expressed in the form of Equation (5):

$$C_p(\lambda,\beta) = 0.5176\times(116\Gamma - 0.4\beta - 5)\times e^{-21\Gamma} + 0.0068\lambda \qquad \forall\Gamma = \frac{1}{\lambda + 0.08\beta} - \frac{0.035}{\beta^3 + 1} \tag{5}$$

Phrase Γ introduces a covariate for calculating (C_p). Moreover, the power of the rotor (aerodynamic power, also denoted as (P_a)) is given by Equation (6):

$$P_a = \omega_r T_a \tag{6}$$

that (T_a) is equal to the aerodynamic torque, and Equation (7) can be calculated by:

$$T_a = \frac{1}{2}\pi\rho R^3 C_q(\lambda) v^2 \tag{7}$$

where (C_q) is calculated based on Equation (8):

$$C_q(\lambda) = \frac{C_p(\lambda)}{\lambda} \tag{8}$$

B) squirrel cage induction generator model (SCIG): Voltage equations of squirrel cage asynchronous generator in dq frame of reference based on references [19-20] can be expressed as Equation (9):

$$\begin{bmatrix} v_{ds} \\ v_{qs} \\ 0 \\ 0 \end{bmatrix} = \begin{bmatrix} R_s + L_s p & -\omega_1 L_s & L_m p & -\omega_1 L_m \\ \omega_1 L_s & R_s + L_s p & \omega_1 L_m & L_m p \\ L_m p & 0 & R_r + L_r p & 0 \\ \omega_s L_m & 0 & \omega_s L_r & R_r \end{bmatrix} \begin{bmatrix} i_{ds} \\ i_{qs} \\ i_{dr} \\ i_{qr} \end{bmatrix} \quad (9)$$

Also, the equations of connected flux are based on [20-21] and can be calculated by Equation (10):

$$\begin{bmatrix} \phi_{ds} \\ \phi_{qs} \\ \phi_{dr} \\ \phi_{qr} \end{bmatrix} = \begin{bmatrix} L_s & 0 & L_m & 0 \\ 0 & L_s & 0 & L_m \\ L_m & 0 & L_r & 0 \\ 0 & L_m & 0 & L_r \end{bmatrix} \begin{bmatrix} i_{ds} \\ i_{qs} \\ i_{dr} \\ i_{qr} \end{bmatrix} \quad (10)$$

Hence, the SCIG torque equation can be calculated by Equation (11):

$$T_e = n_p \frac{L_m}{L_r} i_{qs} \phi_r \quad (11)$$

Additionally, this is described by Equation (12):

$$\phi_r = \frac{L_m}{T_r p + 1} i_{ds} \quad (12)$$

In the aforementioned equations, (v_{ds}) and (v_{qs}) represent the components of the measured voltage; (i_{ds}), (i_{qs}), (i_{dr}), and (i_{qr}) are the respective stator and rotor current components. The vector components of stator and rotor flux linkages are denoted as (ϕ_{ds}), (ϕ_{qs}), (ϕ_{dr}), and (ϕ_{qr}). Stator and rotor phase resistances are indicated by (R_s) and (R_r)respectively. (L_r) and (L_s) correspond to the stator and rotor inductance, while (L_m) signifies the mutual inductance between the stator and rotor. The symbol (n_p) stands for the number of pole pairs, (p) denotes the time derivative $\left((\frac{d}{dt})\right)$, (ω_s) represents the synchronous angular velocity and the rotor time constant $((T_r))$ is expressed as $(\frac{L_r}{R_r})$.

2.2. Proposed sliding mode control

Sliding Mode Control (SMC) has been applied to various systems recently due to its simplicity in implementation and robustness against uncertainties and external disturbances [22]. SMC involves guiding the system to a desired sliding surface and then applying a control law to ensure the system remains within this surface [23]. The design process of SMC includes 1) selecting the sliding surface, 2) specifying the conditions for convergence, and 3) defining the control law for sliding mode, with each step detailed below:

A) Selecting the switching level: A nonlinear system can be be expressed as Equation (13):

$$\dot{X} = f(X,t) + g(X,t)u(X,t) \qquad X \in R^n, u \in R \quad (13)$$

that *f(X,t)* and *g(X,t)* are assumed to be bounded and non-deterministic linear non-continuous functions. Generally, the form of Eq is utilized by Cellutin to determine the sliding surface [24], as presented in the following form, known as Equation (14):

$$S(X)=\left(\frac{d}{dt}+\gamma\right)^{n-1} e, \quad e=X^{d}-X, \quad X=[X,\dot{X},...,X^{n-1}]^{T}, \; X^{d}=[X^{d},\dot{X}^{d},\ddot{X}^{d},...]^{T} \tag{14}$$

where, e, γ, n, X^{d}, and X are equal to the error vector, positive coefficient, system degree, requested state vector, and state vector, respectively.

b) Definition of convergence conditions: Convergence conditions that determine the allowed and non-allowed area are established through the Lyapunov Equation [25] as depicted in Equation (15):

$$S(x)\dot{S}(X)\leq 0 \tag{15}$$

The control algorithm is defined by Equation (16):

$$u=u^{eq}+u^{n} \tag{16}$$

where u, u_{eq}, u^{n}, $sat(S(X)/\varphi)$ and φ are Control variable, equivalent control variable, switching control, saturation function and threshold width of the saturation function respectively. See Equations (17) and (18):

$$u^{n}=u^{\max} sat(S(X)/\varphi) \tag{17}$$

$$sat(S(X)/\varphi)=\begin{cases}\text{sgn}(S) & if \;\; |S|>\varphi \\ S/\varphi & if \;\; |S|<\varphi\end{cases} \tag{18}$$

Based on Equation (12), the rotor flux (φ_r) is solely a function of the d-axis stator current (i_ds). Thus, if the rotor flux remains constant, the generator torque (T_e) depends only on the q-axis stator current (i_qs). Consequently, controlling T_e can be achieved by regulating i_qs. A proposed SMC scheme for controlling the electromagnetic torque (T_e) of a variable speed SCIG wind turbine is illustrated in Figure 3. In the variable speed wind turbine system, the sliding surface is chosen to allow the turbine to operate near the optimal regime characteristics [26]. Therefore, the sliding surface in this study is selected based on Ref. [27] as follows in Equation (19):

$$S=m_1 J_t \omega_h + m_2 J_t T_e - J_t \omega^{*}_{h} \tag{19}$$

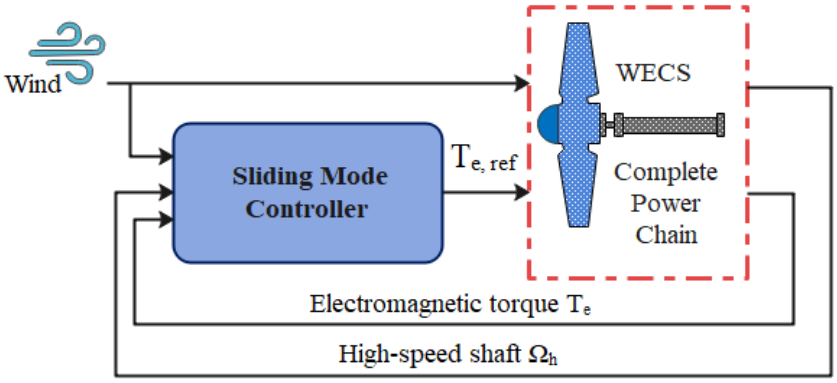

Figure 3. Sliding mode control plan.

The total sliding mode control law for the variable speed wind turbine system is the sum of the equivalent control components and switching control components. This is considered in Equations (20)-(22)

$$T_{e-ref} = u^{eq} + u^{n} \tag{20}$$

$$u^{eq} = T_e - \frac{T_e}{1+m_2 J_t}\left(m_1 J_t \omega_h + m_2 J_t T_e\right)\left(m_1 - A(\lambda, v)\right) \tag{21}$$

$$A(\lambda, v) = \left(K.v.R^2\right)/\, j^2.\left(\dot{C}_p(\lambda).\lambda - C_p(\lambda)\right)/\, \lambda^2 \tag{22}$$

Considering $K = 0.5\pi\rho * R^2$ and $\left(C_P'(\lambda)\right)$ equal to the derivative of the power factor relative to (λ). Also, $(m_1 = -1/T_{sm})$ is equal to the inverse of the time constant, and (m_2) is equal to the static gain. This relationship is presented as Equation (23):

$$m_2 = -m_1 \frac{\omega_{hopt}}{T_{eopt}\left(1+\kappa\left(\omega_h - \omega_{hopt}\right)/\, \omega_{hopt}\right)} \tag{23}$$

The switching component of the control of the sliding law $\left((u_n)\right)$ is determined by selecting the Lyapunov function. The root form of the obtained sliding surface is calculated according to Equation (24):

$$u^{n} = -\alpha\, \mathrm{sgn}_{\varphi}(S) \tag{24}$$

2.3. Particle swarm algorithm (PSO)

To initiate the particle swarm optimization (PSO) algorithm, specific populations are established for each variable. Subsequently, a random value is generated for each variable and population within the predefined range of variable changes. The next phase involves calculating the fitness function for each population, noting that the fitness function aligns with the objective function of the problem at hand. Following this, the algorithm determines the best point, representing the optimum of the fitness function, with the variables at this juncture denoted as (x_{best}). To navigate towards this optimal point, the particle transitions to a new position at a certain velocity. Thus, this stage necessitates the computation of the particle's new velocity and position, achievable through Equations (25) and (26), respectively [28].

$$v_j^{(k+1)} = w v_j^{(k)} + c_1 \times rand_1 \times \left(x_{best}^{(k)} - x_j^{(k)}\right) + c_2 \times rand_2 \times \left(x_{best}^{(k)} - x_j^{(k)}\right) \tag{25}$$

$$x_j^{(k+1)} = x_j^{(k)} + v_j^{(k+1)} \tag{26}$$

In Equation (25), the coefficients (c_1), (c_2), and(w) are recognized as the tuning parameters of the particle swarm optimization algorithm. Modifying these parameters can enhance the algorithm's proficiency in problem-solving at certain points. Typically, based on empirical evidence, suitable values for (c_1), (c_2), and (w) are 2, 2, and 0.7, respectively. This formula indicates that the velocity of each particle is determined by its deviation from the target position. Subsequently, Equation (26) calculates the particle's new location. The subsequent step involves evaluating the fitness function for the new positions of the particles and assessing the convergence criteria. It's important to note that these steps are iteratively refined to achieve convergence. For this study, the

objective function, or fitness criterion, for the particle swarm optimization is defined as the mean squared error (MSE), detailed in Equation (27):

$$MSE = \frac{1}{nT}\sum_{i=1}^{n} e(K)^2 \tag{27}$$

where $(e(k))$ represents the total number of samples, and (T) denotes the sampling time. (e) signifies the deviation between the reference rotor current and its actual value in the (d) direction, the difference between the reference electromagnetic torque and its actual value under Sliding Mode Control (SMC), and the disparity between the reference rotor speed and its actual speed. It is important to highlight that, as illustrated in Figure 2, the output of this process consists of the decision variables, which serve as reference signals for the torque, rotor current, and rotor speed.

3. Numerical results

In this section, the capability of the scheme is investigated. Hence, the case study is introduced first, and then, the obtained results are expressed.

3.1. Study case

The system under consideration is integrated into a 2 MW wind turbine. It's important to note that the characteristics of its generator and the aerodynamic components are detailed in Table 1. Additionally, it is assumed that the turbine experiences no friction, leading to the friction coefficient (K_t) being set to zero. Moreover, the optimal settings for the Particle Swarm Optimization (PSO) algorithm, namely the inertia weight (w), and the acceleration coefficients (c_1) and (c_2), are chosen to be 0.7, 2, and 2, respectively, as per Ref. [23]. The algorithm is configured with a population size of 20 and is set to run for 100 iterations.

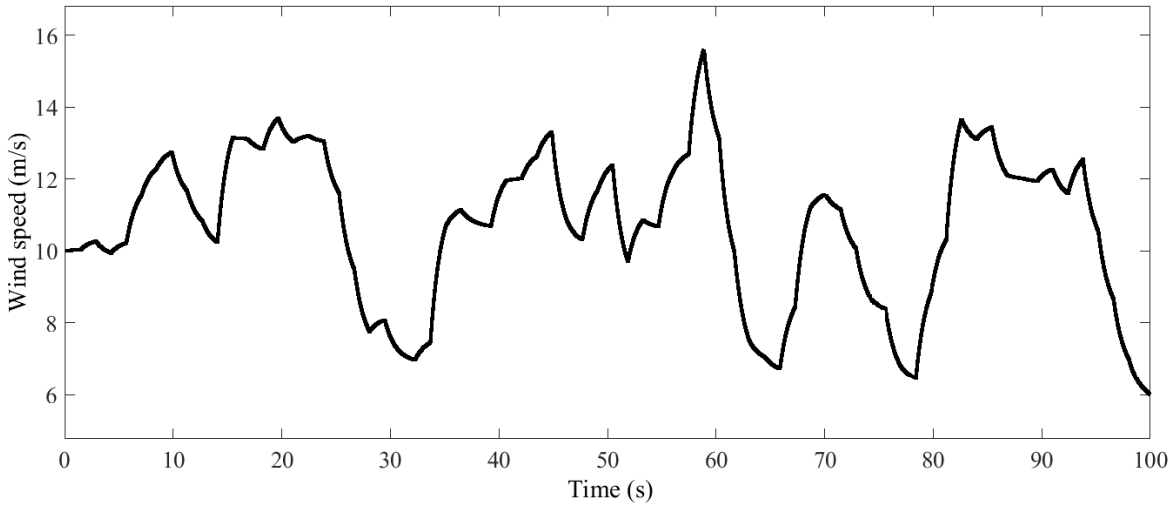

Figure 4. Time graph of wind speed.

Table 1. Wind turbine parameters.

Parameters	Values
K_t	0
J_t	$4.4532 * 10^5 Kgm^2$
ρ	1.225 kg/m^3
R	37.5m
τ_β	0.1

The performance of the wind turbine is significantly influenced by wind speed, making it a critical input parameter. In this study, the wind speed considered for the turbine is depicted in Figure 4. As illustrated, the wind speed fluctuates widely within both high and low-speed ranges, introducing a random element that tests the system's resilience across these conditions. The wind speeds range from 7 to 16 meters per second. It's important to clarify that such variability represents an extreme scenario unlikely to occur in practice. Rapid and severe changes in wind speed are rare in real-life conditions and are employed here solely to assess the robustness of the control system under challenging circumstances.

3.2. Results

The results depicted in Figures 5 to 9 showcase various parameters: the input time curve of the bending angle, bending angle itself, aerodynamic power, aerodynamic torque, turbine absorption coefficient, rotor speed, rotor flux in the q and d directions, generator torque, and the generator output voltage along the d and q axes. An examination of Figure (5-a) and a comparison with Figure 4 reveal that an increase in wind speed, or when the wind speed is notably high, triggers a control input signal for the bending angle, whereas this signal remains zero in conditions of low wind speed.

It is observed from Figure (5-b) that when the bending angle control input signal is engaged or is non-zero, the bending angle changes. This alteration helps in reducing the mechanical stress on the wind turbine, thereby preventing damage to the wind turbine system. Corresponding to the wind speed shown in Figure 4 and the bending angle depicted in Figure (5-b), the daily absorption coefficient curve resembles what is shown in Figure (5-c). From this figure, it is evident that the absorption coefficient consistently registers low values. However, due to variations in wind speed, the absorption coefficient curve is also subject to change over time. Nonetheless, as illustrated in Figures (5-d) and (5-e), the wind turbine exhibits high aerodynamic power and torque. It is important to note that, in many instances, the rotor speed difference relative to its reference speed diminishes, as shown in Figure 6.

Figures (7-a) and (7-b) display the rotor current curves in the q and d directions, respectively. It is important to note that the current in the d direction correlates with the reactive power of the turbine, which remains constant regardless of wind speed; hence, the rotor current in the d direction remains constant. Conversely, the flow in the q direction is tied to the aerodynamic power and, thus, varies in accordance with wind

speed. Consequently, the generator's output active power, which depends on the rotor current in the q direction, also fluctuates over time, as depicted in Figure 8. The last graph showcases the stator voltage in the d and q directions, presented in Figure 9.

From the figure, it's evident that the output voltage fluctuates over time, reflecting variations in wind speed. This phenomenon is attributed to the need for the rotor current in the q-direction to align closely with its reference signal, minimizing the error rate.

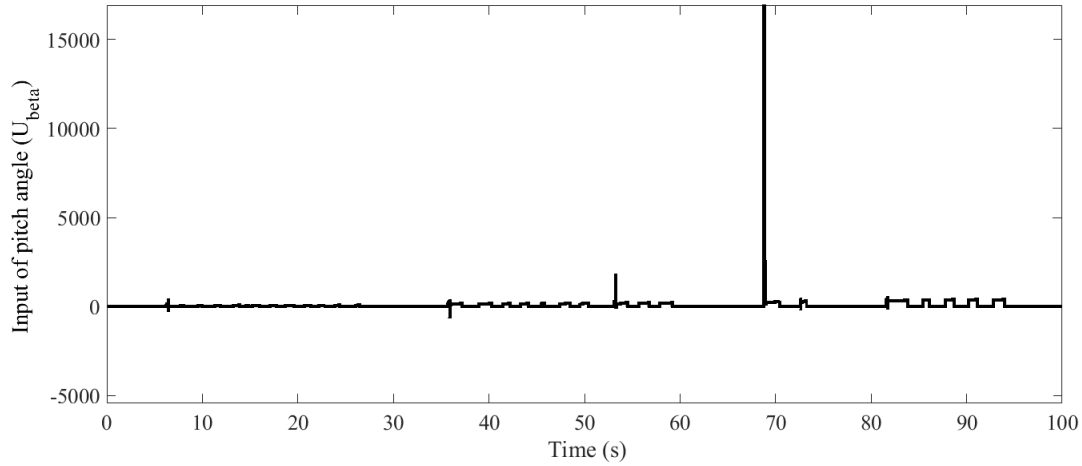

(a)

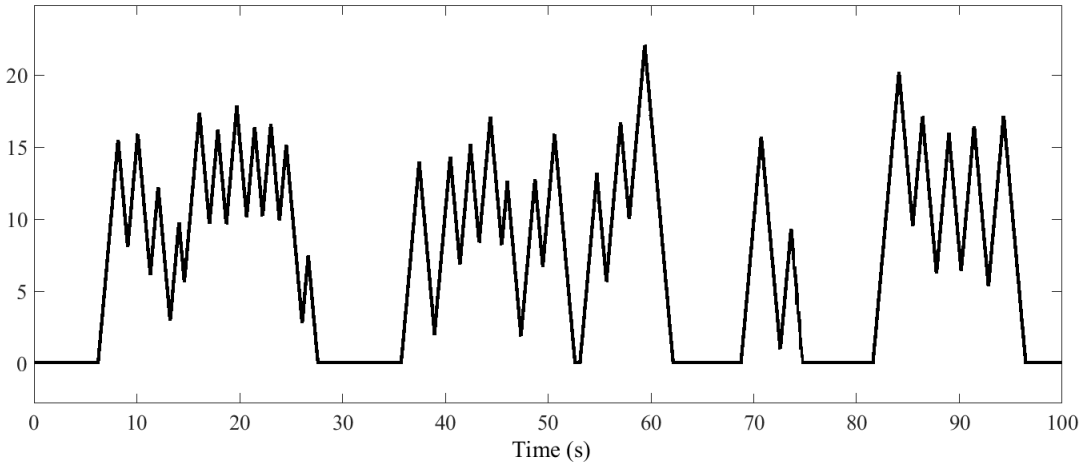

(b)

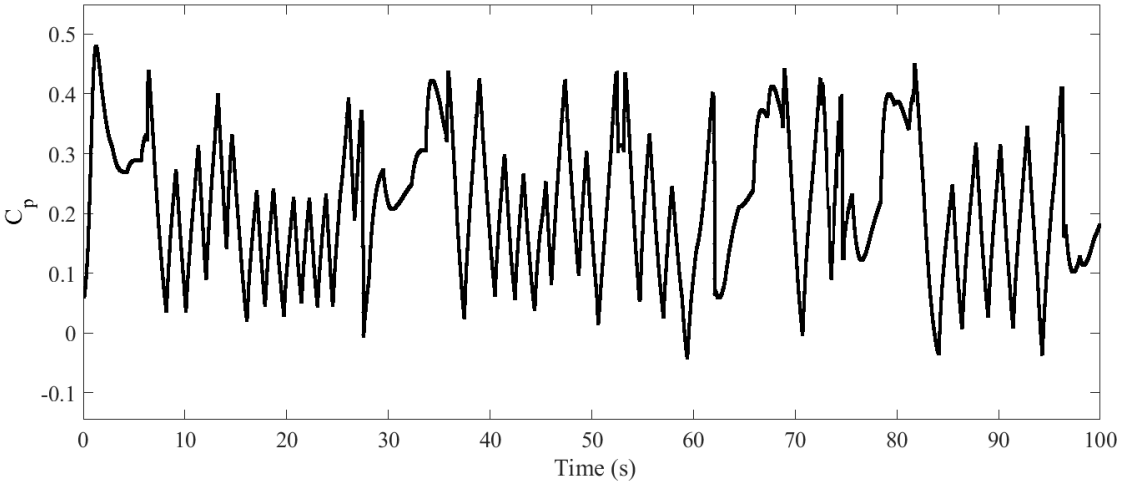

(c)

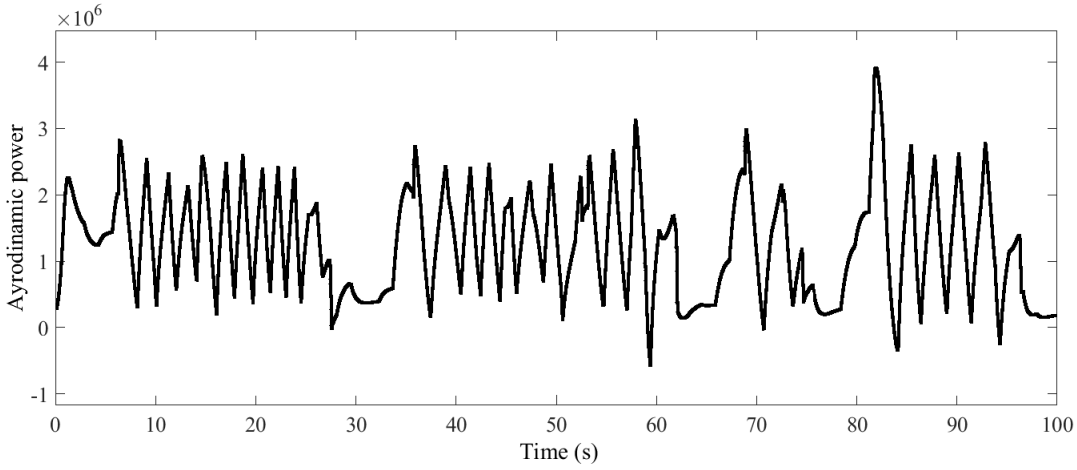

(d)

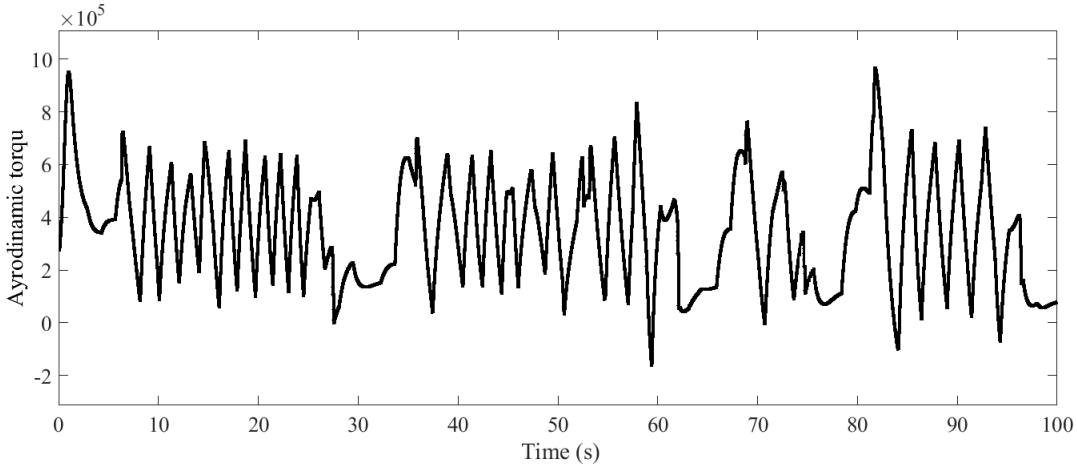

(e)

Figure 5. Time diagram, a) Bending angle input, b) Bending angle, c) Turbine absorption coefficient, d) Turbine aerodynamic power, e) Turbine aerodynamic torque.

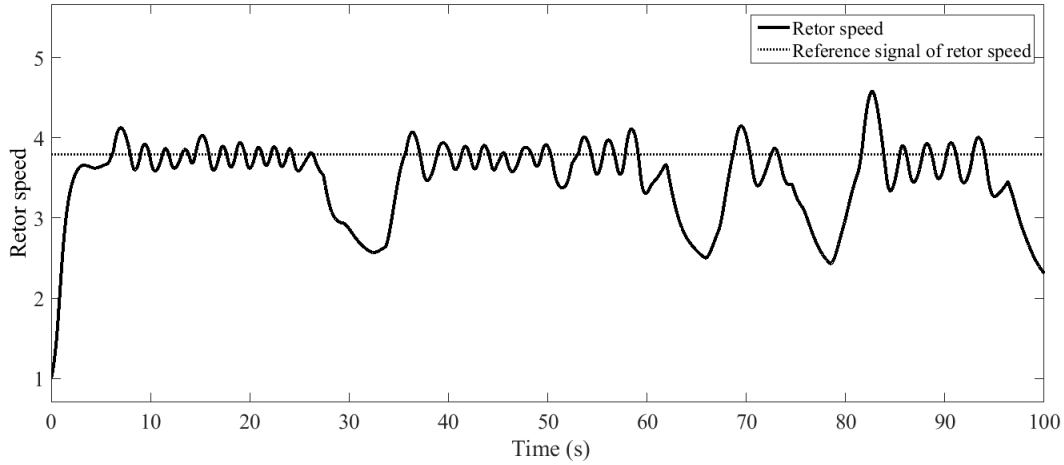

Figure 6. Time graph of real speed and rotor reference.

Consequently, the reference signal for the rotor current in the q-direction changes with wind speed, necessitating adjustments in the rotor current to match wind speed fluctuations. This adjustment leads to changes in the generator's output voltage.

Table 2 details the mean square error deviations for the control strategies under review: one employing solely sliding mode control and another combining sliding mode control with the PSO algorithm. The data indicate that the mean square error is significantly reduced in the design that integrates sliding mode control with the PSO algorithm, showcasing a notable advantage of the proposed design.

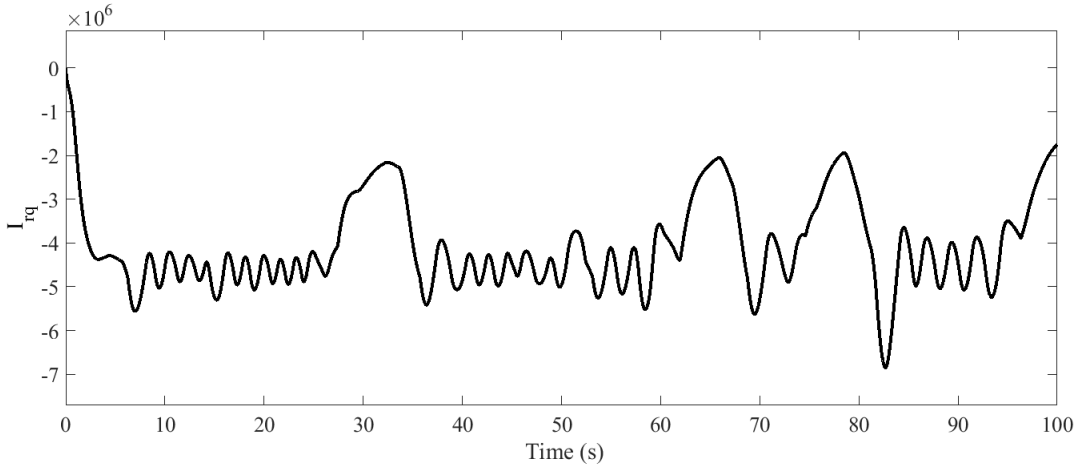

(a)

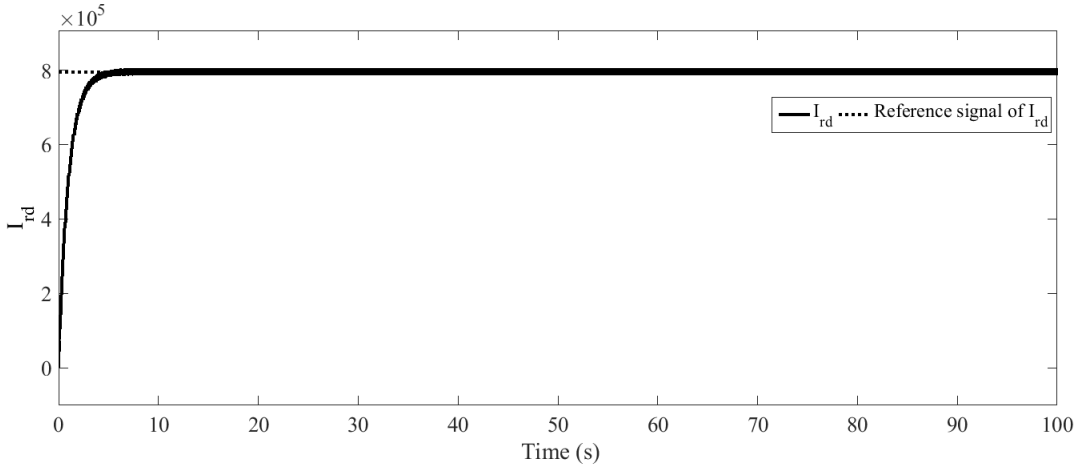

(b)

Figure 7. Time diagram, a) rotor current in direction q, b) rotor current in direction d.

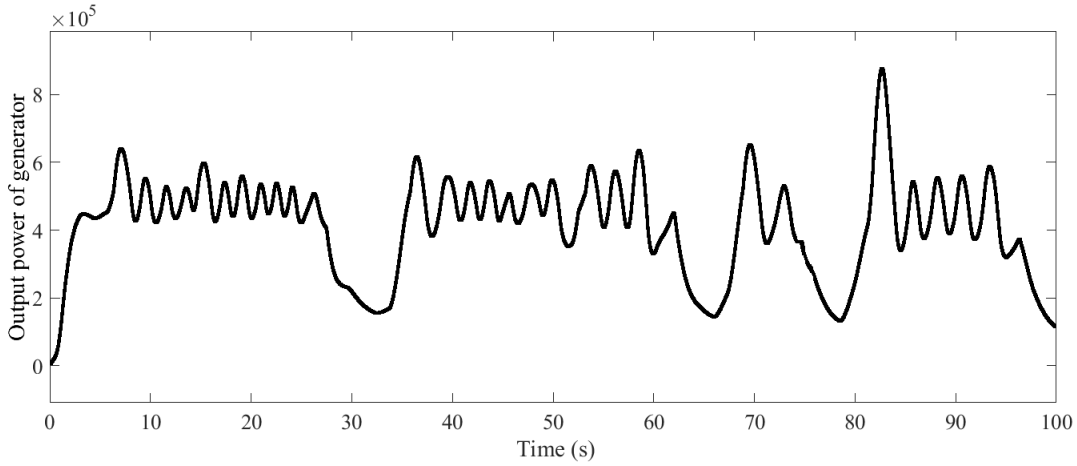

Figure 8. Time diagram of active generator power.

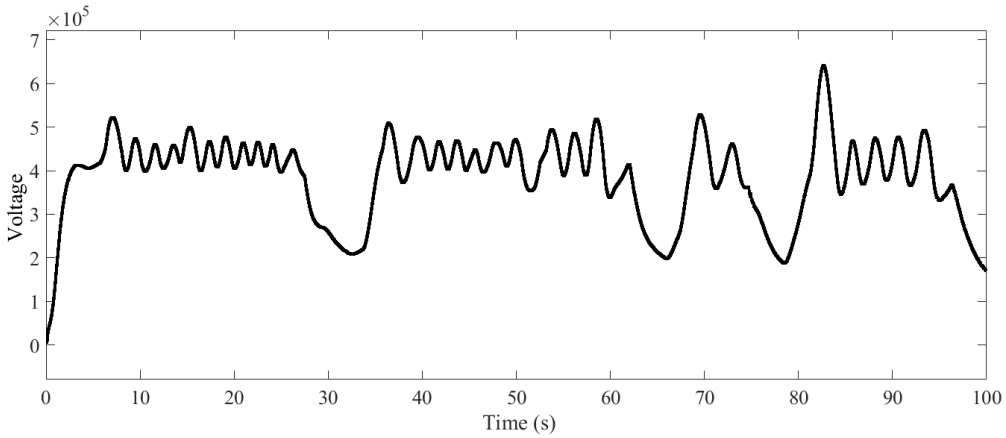

(a)

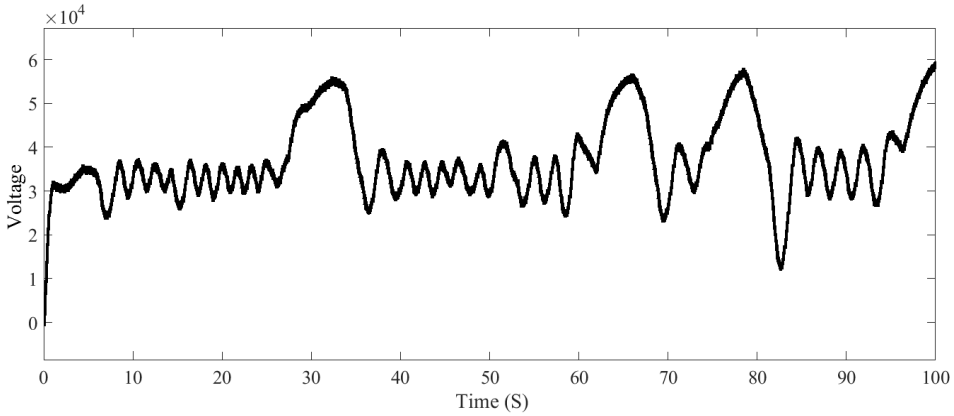

(b)

Figure 9. Time diagram of the output voltage of the stator, a) in the direction of d, b) in the direction of q.

Table 2. Mean square error deviations for different study cases.

Level	Study case
34/12	Proposed design with sliding mode control
57/8	The proposed combination of sliding mode control and PSO algorithm

4. Conclusion

In this paper, the wind turbine model is a combination of sliding mode and PSO algorithm. In the turbine model, the aerodynamic part and its generator were considered. Then the first-order sliding mode controller was presented on the proposed system. Finally, the PSO was applied to minimize the error correction between the reference signal of the control variables and the variables themselves. Then, the proposed problem was applied to a standard wind turbine and based on the numerical results, the following general results were obtained:

- Increasing blade bending angle at high-speed winds to reduce mechanical stress and damage mechanical flexibility
- The input signal of bending angle control at speed is zero the low wind was due to the lack of high mechanical pressure

- The low absorption coefficient of the wind turbine due to the proper control of the blade bending angle at speed upwind
- Changes in aerodynamic power and moment proportional to time and their dependence on wind speed and blade bending angle I see
- Excellent tracking of the rotor current in the *q* direction with minimal error when using a combination of sliding mode control and PSO algorithm
- Excellent tracking of the rotor current in the *d* direction with minimal error when using a combination of sliding mode control and PSO
- Dependence of the rotor current in the *q* direction on the wind speed due to the dependence of the rotor current in the *q* direction on the active generator power
- The lack of dependence of the rotor current in the *d* direction on the wind speed is due to the dependence of the rotor current in the *d* direction on the reactive power of the generator.
- Generator output voltage changes proportional to wind speed to properly control the rotor current in *q* and *d* directions
- A low mean square error (MSE) if a combination of sliding mode control and PSO algorithm is adopted.

References

[1] H. Liang, and S. Pirouzi, "Energy Management System Based on Economic Flexi-Reliable Operation for the Smart Distribution Network Including Integrated Energy System of Hydrogen Storage and Renewable Sources," *Energy*, vol. 293, 130745, 2024.

[2] F. Khalafian, and N. Iliaee, et al., "Capabilities of Compressed Air Energy Storage in the Economic Design of Renewable Off-Grid System to Supply Electricity and Heat Costumers and Smart Charging-Based Electric Vehicles," *Journal of Energy Storage*, vol. 78, pp. 109888, 2024.

[3] S. Pirouzi, "Network-Constrained Unit Commitment-Based Virtual Power Plant Model in the Day-Ahead Market According to Energy Management Strategy," *IET Generation, Transmission & Distribution*, vol. 17, no. 22, pp. 4958-4974, 2023.

[4] B. Wu, Y. Lang, N. Zargari, and S. Kouro, "*Power Conversion and Control of Wind Energy Systems,*" vol. 74. John Wiley & Sons, 2011.

[5] E. Strantzali, and K. Aravossis, "Decision Making in Renewable Energy Investments: A Review," *Renewable and Sustainable Energy Reviews*, vol. 55, pp. 885-898, 2016.

[6] L. Wang, R. Bergua, et al., "Experimental Investigation of Advanced Turbine Control Strategies and Load-Mitigation Measures with a Model-Scale Floating Offshore Wind Turbine System," *Applied Energy*, vol. 355, pp. 122343, 2024.

[7] N. J. Abbas, J. Jasa, D. S. Zalkind, A. Wright, and L. Pao, "Control Co-Design of a Floating Offshore Wind Turbine," *Applied Energy*, vol. 353, pp. 122036, 2024.

[8] S. Saravanan, and N. R. Babu, "Maximum Power Point Tracking Algorithms for Photovoltaic System–A Review," *Renewable and Sustainable Energy Reviews*, vol. 57, pp. 192-204, 2016.

[9] B. Beltran, M. E. H. Benbouzid, and T. Ahmed-Ali, "High-Order Sliding Mode Control of a Dfig-Based Wind Turbine for Power Maximization and Grid Fault Tolerance," *IEEE International Electric Machines and Drives Conference*, pp. 183-189, 2009.

[10] B. Beltran, T. Ahmed-Ali, and M. E. H. Benbouzid, "High-Order Sliding-Mode Control of Variable-Speed Wind Turbines," *IEEE Transactions on Industrial Electronics*, vol. 56, no. 9, pp. 3314-3321, 2008.

[11] X. Yang, and X. Liu, "Integral Variable Structure Fuzzy Adaptive Control for Variable Speed Wind Power System," *International Conference on Logistics Systems and Intelligent Management (ICLSIM)*, vol. 2, pp. 1247-1250, 2010.

[12] O. A. Morfin, A. G. Loukianov, J. M. Cañedo, and M. I. Castellanos, "Velocity Controller of a Wound Rotor Induction Generator via Block Control Linearization-Second Order Sliding Modes," *International Conference on Electrical Engineering Computing Science and Automatic Control*, pp. 77-82, 2010.
[13] C. Evangelista, F. Valenciaga, and P. Puleston, "Active and Reactive Power Control for Wind Turbine Based on a MIMO 2-Sliding Mode Algorithm with Variable Gains," *IEEE Transactions on Energy Conversion*, vol. 28, no. 3, pp. 682-689, 2013.
[14] G. L. Hou, R. Wang, and J. Zhang, "The Application of Integral Variable Structure Control in Cutting-in Control of Double-Fed Induction Generator," *2009 4th IEEE Conference on Industrial Electronics and Applications,* pp. 3152-3157, 2009.
[15] L. Zhang, E. Chunliang, H. Li, and H. Xu, "A New Pitch Control Strategy for Wind Turbines Base on Quasi-Sliding Mode Control," *2009 International Conference on Sustainable Power Generation and Supply*, pp. 1-4, 2009.
[16] X. Fei, H. X. Wang, and M. Chen, "A Novel Sensorless Control of PMSG Based on Sliding Mode Observer," *The XIX International Conference on Electrical Machines - ICEM 2010,* pp. 1-4, 2010.
[17] L. Shang, and J. Hu, "Sliding-Mode-Based Direct Power Control of Grid-Connected Wind-Turbine-Driven Doubly Fed Induction Generators Under Unbalanced Grid Voltage Conditions," *IEEE Transactions on Energy Conversion, vol. 27, no. 2, pp. 362-373,* 2012.
[18] Y. Kumar, J. Ringenberg, et al., "Wind Energy: Trends and Enabling Technologies," *Renewable and Sustainable Energy Reviews*, vol. 53, pp. 209-224, 2016.
[19] A. Luque, and S. Hegedus, "*Handbook of Photovoltaic Science and Engineering"*. John Wiley & Sons, 2011.
[20] H. Kobayashi, and H. Hatta, "Reactive Power Control Method Between DG Using ICT for Proper Voltage Control of Utility Distribution System," *IEEE Power and Energy Society General Meeting*, pp. 1-6, 2011.
[21] F. Blaabjerg, M. Liserre, and K. Ma, "Power Electronics Converters for Wind Turbine Systems," *IEEE Energy Conversion Congress and Exposition*, pp. 281-290, 2012.
[22] Y. Soufi, S. Kahla, and M. Bechouat, "Particle Swarm Optimization Based Sliding Mode Control of Variable Speed Wind Energy Conversion System," *International Journal of Hydrogen Energy*, vol. 41, no. 45, pp. 20956-20963, 2016.
[23] K. Tan, and S. Islam, "Optimal Control Strategies in Energy Conversion of PMSG Wind Turbine System Without Mechanical Sensors," *IEEE Transactions on Energy Conversion*, vol. 19, no. 2, pp. 392-399, 2004.
[24] J. M. Carrasco, L. G. Franquelo, et al., "Power-Electronic Systems for the Grid Integration of Renewable Energy Sources: A Survey," *IEEE Transactions on Industrial Electronics*, vol. 53, no. 4, pp. 1002-1006, 2006.
[25] D.K. Fidaros, C.A. Baxevanou, T. Bartzanas, and C. Kittas, " Numerical Simulation of Thermal Behavior of a Ventilated Arc Greenhouse During a Solar Day," *Renewable Energy*, vol. 35, no.7, 2010.
[26] R. Pena, J. C. Clare, and G. M. Asher, "Doubly Fed Induction Generator Using Back-to-Back PWM Converters and its Application to Variable-Speed Wind-Energy Generation," *IEE Proceedings - Electric Power Applications*, vol. 143, no. 3, pp. 231-241, 1996.
[27] I. Munteanu, A. I. Bratcu, E. Ceanga, and N.A. Cutululis, "Optimal Control of Wind Energy Systems"*, Towards a Global Approach*, vol. 22, p. 286. London: Springer, 2008.
[28] Y. Del Valle, G. K. Venayagamoorthy, S. Mohagheghi, J. C. Hernandez, and R. G. Harley, "Particle Swarm Optimization: Basic Concepts, Variants and Applications in Power Systems," *IEEE Transactions on Evolutionary Computation*, vol. 12, no. 2, pp. 171-195, 2008.

Declaration of Competing Interest

The authors declare that they have no known competing financial interests or personal relationships that could have appeared to influence the work reported in this paper. The ethical issues, including plagiarism, informed consent, misconduct, data fabrication and/or falsification, double publication and/or submission, redundancy, have been completely observed by the authors.

Credit Authorship Contribution Statement

Sasan Pirouzi: Conceptualization, Formal analysis, Project administration, Supervision, Validation, Roles/Writing - original draft. **Ali Naderi:** Conceptualization, Investigation, Methodology, Resources, Visualization, Writing - review & editing.

Bibliography

Sasan Pirouzi received a BSc degree in electrical engineering from the Technical and Vocational University, Mashhad, Iran, in 2012 and an MSc degree from the Isfahan University of Technology, Isfahan, Iran, in 2014, as well as a PhD from the Shiraz University of Technology (SUTECH), Shiraz, Iran, in 2017. His research interests are power system operation and planning, electric vehicles, DERs and the application of optimization methods in power systems.

Ali Naderi was born in Iran. He is currently a master's student in the field of electrical engineering at Yazd University. His special interests are operation and planning of power systems.